ME555: Course Project Report

Topology optimisation of micro-mirror actuator

Submitted by

UMID	Names of Students
8986 8250	Geetha Krishna
5437 2155	Mayur Birla

Under the guidance of
Dr Emrah Bayrak

University of Michigan, Ann Arbor
Michigan, USA-48109

Winter Semester 2016

Contents

List of Figures

List of Tables

1 Introduction

1.1 Project overview

The Endoscope is a vital instrument in tissue imaging. The image is generated by raster scanning principle where the pixel level data is gathered by focusing the laser beam on the tissue. The scanning of laser beam, at different depths, is carried out by providing motion to the micro-mirror attached to compliant mechanism involving PZT (Lead Zirconate Titanate) material to actuate it. The micro-mirror is desired to have maximum possible out-of-plane displacement (U_z) for getting data at larger depths. The maximum displacement i.e more compliant structure is limited by the ability to micro-fabricate the minimum feature size (b) Also, the mirror is desired to have high natural frequency (ω) or faster performance. So the objective of our project is to optimize the topology of complaint mechanism to get maximum displacement along with high frequency.

At system level we need to maximize U_z with given boundary conditions, subjected to lower bound on natural frequency and minimum feature size. So at subsystem level 1 we will be maximizing the U_z subjected to constraint on minimum feature size only. At subsystem level 2 we want to maximize the natural frequency subjected to constraint on minimum displacement.

System-level objective

$$\begin{aligned} \text{max:} \quad & U_z(B) \cdot \omega^2 \\ \text{subjected to:} \quad & \text{volume} \leq \text{volume}^* \end{aligned} \tag{1.1}$$

Sub-system1 objective

$$\begin{aligned} \text{max:} \quad & U_z(B) \\ \text{subjected to:} \quad & \text{volume} \leq \text{volume}^* \end{aligned} \tag{1.2}$$

Sub-system2 objective

$$\begin{aligned} \text{max:} \quad & \omega^2 \\ \text{subjected to:} \quad & \text{volume} \leq \text{volume}^* \end{aligned} \tag{1.3}$$

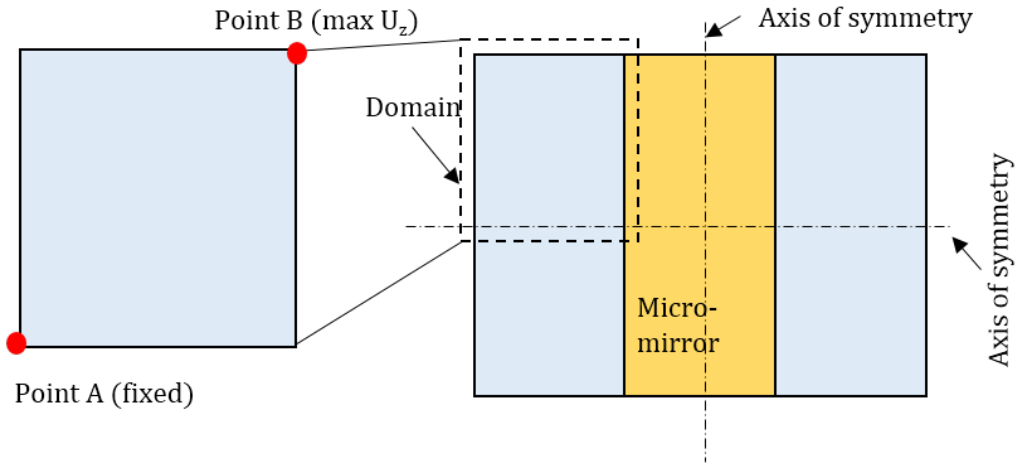

Figure 1.1: Micro-mirror and actuator domain

2 Model

2.1 Finite Element Methods

The symmetricity of the problem about X and Y axis (refer fig. 1.1) allows us to consider a quarter of the domain for optimization purposes. The result obtained can then be extended to the complete domain. The optimization of this domain first requires developing a mathematical model for analysis.

As we need to analyze properties like frequencies and displacements, this leads us to develop simulation models through which the objectives and required variables can be calculated. The simulation models for structures are best represented by Finite Element Methods. So we develop models for optimization using FEM.

The basic building block of FEM is an element whose characteristic properties are well established. Depending upon our requirement, particular element type can be chosen for representing our domain and this leads us in building the mathematical model to represent our physical structure.

The immense variety of elements allows us to carefully choose a particular type for mathematically representing the domain. Say, our domain can be represented by 2D triangular elements, 2D Quadrilateral elements and even it can be modelled by 1D elements with proper connectivity so that it is represented aptly.

To start with, we have chosen 1D elements with two nodes each having 6 DOF $[U_x \quad U_y \quad U_z \quad \theta_x \quad \theta_y \quad \theta_z]$, three in translation and three in rotation. Further we can always switch to more eloborate and accurate description by modelling it with 2D or 3D elements.

The element stiffness and mass matrix for 2 node 12 DOF frame element are given below:

2.2 Element Stiffness matrix

$$\mathbf{k}_i = \begin{bmatrix}
\frac{EA}{L} & 0 & 0 & 0 & 0 & 0 & \frac{-EA}{L} & 0 & 0 & 0 & 0 & 0 \\
0 & \frac{12EI_z}{L^3} & 0 & 0 & 0 & \frac{6EI_z}{L^2} & 0 & \frac{-12EI_z}{L^3} & 0 & 0 & 0 & \frac{6EI_z}{L^2} \\
0 & 0 & \frac{12EI_y}{L^3} & 0 & \frac{-6EI_y}{L^2} & 0 & 0 & 0 & \frac{-12EI_y}{L^3} & 0 & \frac{-6EI_y}{L^2} & 0 \\
0 & 0 & 0 & \frac{GJ}{L} & 0 & 0 & 0 & 0 & 0 & \frac{-GJ}{L} & 0 & 0 \\
0 & 0 & \frac{-6EI_y}{L^2} & & \frac{4EI_y}{L} & 0 & 0 & 0 & \frac{6EI_y}{L^2} & 0 & \frac{2EI_y}{L} & 0 \\
0 & \frac{6EI_z}{L^2} & 0 & 0 & 0 & \frac{4EI_z}{L} & 0 & \frac{-6EI_z}{L^2} & 0 & 0 & 0 & \frac{2EI_z}{L} \\
\frac{-EA}{L} & 0 & 0 & 0 & 0 & 0 & \frac{EA}{L} & 0 & 0 & 0 & 0 & 0 \\
0 & \frac{-12EI_z}{L^3} & 0 & 0 & 0 & \frac{-6EI_z}{L^2} & 0 & \frac{12EI_z}{L^3} & 0 & 0 & 0 & \frac{-6EI_z}{L^2} \\
0 & 0 & \frac{-12EI_y}{L^3} & 0 & \frac{6EI_y}{L^2} & 0 & 0 & 0 & \frac{12EI_y}{L^3} & 0 & \frac{6EI_y}{L^2} & 0 \\
0 & 0 & 0 & \frac{-GJ}{L} & 0 & 0 & 0 & 0 & 0 & \frac{GJ}{L} & 0 & 0 \\
0 & 0 & \frac{-6EI_y}{L^2} & 0 & \frac{2EI_y}{L} & 0 & 0 & 0 & \frac{6EI_y}{L^2} & 0 & \frac{4EI_y}{L} & 0 \\
0 & \frac{6EI_z}{L^2} & 0 & 0 & 0 & \frac{2EI_z}{L} & 0 & \frac{-6EI_z}{L^2} & 0 & 0 & 0 & \frac{4EI_z}{L}
\end{bmatrix}$$

2.3 Element Mass matrix

$$\mathbf{m}_i = \rho AL \begin{bmatrix}
\frac{1}{3} & 0 & 0 & 0 & 0 & 0 & \frac{1}{6} & 0 & 0 & 0 & 0 & 0 \\
0 & \frac{13}{35} & 0 & 0 & 0 & \frac{11L}{210} & 0 & \frac{9}{70} & 0 & 0 & 0 & \frac{-13L}{420} \\
0 & 0 & \frac{13}{35} & 0 & \frac{-11L}{210} & 0 & 0 & 0 & \frac{9}{70} & 0 & \frac{13L}{420} & 0 \\
0 & 0 & 0 & \frac{I_x}{3A} & 0 & 0 & 0 & 0 & 0 & \frac{I_x}{6A} & 0 & 0 \\
0 & 0 & \frac{-11L}{210} & & \frac{L^2}{105} & 0 & 0 & 0 & \frac{-13L}{420} & 0 & \frac{-L^2}{140} & 0 \\
0 & \frac{11L}{210} & 0 & 0 & 0 & \frac{L^2}{105} & 0 & \frac{13L}{420} & 0 & 0 & 0 & \frac{-L^2}{140} \\
\frac{1}{6} & 0 & 0 & 0 & 0 & 0 & \frac{1}{3} & 0 & 0 & 0 & 0 & 0 \\
0 & \frac{9}{70} & 0 & 0 & 0 & \frac{13L}{420} & 0 & \frac{13}{35} & 0 & 0 & 0 & \frac{-11L}{210} \\
0 & 0 & \frac{9}{70} & 0 & \frac{-13L}{420} & 0 & 0 & 0 & \frac{13}{35} & 0 & \frac{11L}{210} & 0 \\
0 & 0 & 0 & \frac{I_x}{6A} & 0 & 0 & 0 & 0 & 0 & \frac{I_x}{3A} & 0 & 0 \\
0 & 0 & \frac{13L}{420} & 0 & \frac{-L^2}{140} & 0 & 0 & 0 & \frac{11L}{210} & 0 & \frac{L^2}{105} & 0 \\
0 & \frac{-13L}{420} & 0 & 0 & 0 & \frac{-L^2}{140} & 0 & \frac{-11L}{210} & 0 & 0 & 0 & \frac{L^2}{105}
\end{bmatrix}$$

3 Optimisation strategy

3.1 Design variable

The subsystem-1 optimizes the topology for having maximum displacement at a particular point and the subsystem-2 optimizes for having maximum natural frequency for the body. The base geometry for both the subsystem is the same and both the subsystem uses same FEA formulation as the design model.

As the design mathematical model being the same, the design variables which are associated with each and every element in the 1D discretized domain remains the same for both the subsystems.

We choose our design variables as Youngs' modulus $E = x_i \mathrm{E}_0$, where E_0 is the actual Youngs' modulus of beam material and x_i can take any value between 0 and 1. x_i's are associated with the each beam element in the discretized model and its value tells us about the importance of the associated element. The element whose x_i is close to 0 can be removed (implying that it is not important) and x_i close to 1 shall remain in the structure (implying that it is vital). Substituting $x_i \mathrm{E}_0$ in the elemental stiffness matrix modifies it as $x_i \mathbf{k}_i$, where $\mathbf{k}_i$ is given in chapter 2. The addition or deletion of the beam element based on the design variable x_i also affect the mass of the system and thereby natural frequency of the structure. Thus, it is important to include the effect of design variable in the mass matrix. This effect can be handled by modelling the density of the element as $\rho = x_i \rho_0$ and which thereby modifies the elemental mass matrix as $x_i \mathbf{m}_i$.

The lower bound $x_i \geq 0$ may lead to singularity of the stiffness and mass matrix, if any $x_i = 0$ which will create numerical issues during FEM analysis. This problem can be circumvented if lower bound is fixed to some small value x^{min} instead of 0. Thus the constraints for lower and upper bounds of design variables becomes

$$x^{min} - x_i \leq 0 \tag{3.1}$$

$$x_i - 1 \leq 0. \tag{3.2}$$

Based on the SIMP (Solid Isotropic Material with Penalization) formulation we can introduce a exponent p for x_i and rewrite the design variable as $x_i^p \mathrm{E}_0$. The higher value of p will push the design variable to its extreme value i.e 0 or 1. Since the extent to which the design variable affects $\mathbf{k}_i$ and $\mathbf{m}_i$ is not same, we incorporate two different SIMP parameters as p and q associated with $\mathbf{k}_i$ and $\mathbf{m}_i$ respectively. For the bending analysis the exponent p and q are typically set to 3 and 1 respectively. During this project we also study the effect SIMP parameters on the optimization results. This is discussed in the results section.

3.2 Volume Constraint

Generally, in topology optimization the intended objective has to be achieved with the limited material due to several possible reasons. It may be due to the space availability, the allowable weight, or due to the cost of the material involved. This imposes additional constraint on total volume of the system. In our case, we use volume constraint to push the results towards less complex geometry for easy manufacturing using micro-fabrication techniques. The design variable which tells us about the amount of material present is an indicator of the volume of the particular element. So we impose the volume constraint as

$$\sum x_i \leq V_f \cdot \text{nelem} \tag{3.3}$$

where nelem is the total number of elements at beginning of optimisation, and V_f is the volume fraction that can take any value from 0 to 1. The volume fraction is a parameter that can be varied to get the best possible result on the expense of volume constraint. A post-optimisation analysis is carried out to study the sensitivity of the constraint. It tells us the relative change in the objective function on changing the constraint value.

3.3 Sub-system 1

Our aim is to maximize U_z at a specified point B, subjected to given constraints. This requires the structure to be more compliant, which allows us to increase the displacement at B, at the same time the topology should be rigid enough to support the weight of the micro-mirror. The displacement at B can be expressed such that it is equal to Mutual Potential Energy (MPE), and the total Strain Energy (SE) can serve as a indicator to rigidity. Thus, the multicriteria objective function can be reformulated as proposed by Saxena et al.[1] given in eq. (3.4), where we maximise the MPE and minimise the

SE. The upper and lower bound on design variable as discussed in section 3.1 serves as constraints in the optimisation problem.

$$\text{minimise:} \quad -\frac{MPE}{SE} \tag{3.4}$$

$$\text{subjected to:} \quad x^{min} - x_i \leq 0 \tag{3.5}$$

$$x_i - 1 \leq 0 \tag{3.6}$$

The MPE and SE can be formulated using FEM as discussed in chapter 2.

$$MPE = \mathbf{V^T K U} \tag{3.7}$$

$$SE = \frac{1}{2}\mathbf{U^T K U} \tag{3.8}$$

Where, $\mathbf{K}$ is the global stiffness matrix, $\mathbf{U}$ is the nodal displacement due to all input forces ($\mathbf{F}$), and $\mathbf{V}$ is the nodal displacement due to unit dummy load ($\mathbf{F_d}$) applied at point B in the direction of desired displacement.(Δ_{out}). $\mathbf{U}$ and $\mathbf{V}$ can be solved by the following equations.

$$\mathbf{KU} = \mathbf{F} \tag{3.9}$$

$$\mathbf{KV} = \mathbf{F_d} \tag{3.10}$$

The Lagrange can be formulated as

$$L = -\frac{MPE}{SE} + \sum \mu_i^{min}(x^{min} - x_i) + \sum \mu_i^{max}(x_i - 1) \tag{3.11}$$

Taking gradient of Lagrange wrt x_i results in

$$\frac{\partial L}{\partial x_i} = \frac{MPE}{SE^2}\frac{\partial (SE)}{\partial x_i} - \frac{1}{SE}\frac{\partial (MPE)}{\partial x_i} + \mu_i^{max} - \mu_i^{min} \tag{3.12}$$

Using eqs. (3.9) and (3.10) Saxena et al. [1] showed that,

$$\frac{\partial (MPE)}{\partial x_i} = -\mathbf{V^T}\frac{\partial \mathbf{K}}{\partial x_i}\mathbf{U}. \tag{3.13}$$

Since each element stiffness matrix $\mathbf{k}_i$ depends only on the i-th design variable, we can simplify the term $\partial \mathbf{K}/\partial x_i$ as $\partial \mathbf{k}_i/\partial x_i$.

$$\frac{\partial (MPE)}{\partial x_i} = -\mathbf{v}^t\frac{\partial \mathbf{k}_i}{\partial x_i}\mathbf{u}. \tag{3.14}$$

By similar argument we can write $\partial (SE)/\partial x_i$ as

$$\frac{\partial (SE)}{\partial x_i} = -\frac{1}{2}\mathbf{u}^t\frac{\partial \mathbf{k}_i}{\partial x_i}\mathbf{u}. \tag{3.15}$$

Now, we can have either lower bound or upper bound, but not both, as an active constraint for a particular design variable. Also, if any one of the constraint is active then the design variable becomes either x^{min} or 1. If non of the contraint is active the design variable is updated using gradient as given below

$$\frac{\partial L}{\partial x_i} = \frac{MPE}{SE^2}\frac{\partial (SE)}{\partial x_i} - \frac{1}{SE}\frac{\partial (MPE)}{\partial x_i}. \tag{3.16}$$

Henceforth we omit the terms μ_i^{max} and μ_i^{min} from the gradient of Lagrange for convenience. By using eqs. (3.14) and (3.15) we rewrite eq. (3.16) as

$$\frac{\partial L}{\partial x_i} = -\frac{MPE}{2SE^2}\mathbf{u}^t\frac{\partial \mathbf{k}_i}{\partial x_i}\mathbf{u} + \frac{1}{SE}\mathbf{v}^t\frac{\partial \mathbf{k}_i}{\partial x_i}\mathbf{u}. \tag{3.17}$$

We employ gradient method to update the design variable as

$$x_i^{k+1} = x_i^k - \alpha\frac{\partial L}{\partial x_i} \tag{3.18}$$

where, α is a line-search parameter.

The objective function given in eq. (3.4) can be formulate in more general way as as proposed by Saxena et al. [1]

$$\text{minimise:} \qquad -\frac{f(MPE)}{g(SE)}, \tag{3.19}$$

where $f(MPE)$ and $g(SE)$ is any monotonically increasing function of MPE and SE repectively. We can rewrite the Lagrange given in eq. (3.11) using aforementioned general objective function and take gradient as

$$\begin{aligned}\frac{\partial L}{\partial x_i} &= -\frac{f'(MPE)}{g(SE)}\frac{\partial (MPE)}{\partial x_i} + \frac{f(MPE)\cdot g'(SE)}{g^2(SE)}\frac{\partial (SE)}{\partial x_i} \\ &= \frac{f'(MPE)}{g(SE)}\mathbf{v}^t\frac{\partial \mathbf{k}_i}{\partial x_i}\mathbf{u} - \frac{f(MPE)\cdot g'(SE)}{2g^2(SE)}\mathbf{u}^t\frac{\partial \mathbf{k}_i}{\partial x_i}\mathbf{u}\end{aligned}$$

For our study, we have chosen the monotonic function f and g as exponent of MPE and SE i.e $f(MPE) = MPE^m$ and $g(SE) = SE^n$. Since SE is always non-negative, any positive real value of n will make g monotonic. However, for f m should always be an even integers. Thus, the gradient of lagrange becomes:

$$\frac{\partial L}{\partial x_i} = \frac{m\cdot(MPE)^{m-1}}{(SE)^n}\mathbf{v}^t\frac{\partial \mathbf{k}_i}{\partial x_i}\mathbf{u} - \frac{n\cdot(MPE)^m}{(SE)^{n+1}}\mathbf{u}^t\frac{\partial \mathbf{k}_i}{\partial x_i}\mathbf{u}. \tag{3.20}$$

This gradient coupled with robust line-search is used to update the design variable as given in eq. (3.18).

3.4 Sub-system 2

Our aim in this subsystem is to maximize the natural frequency of the structure subjected to the given constraints. Maximizing the natural frequency implies that we need a stiff system as opposed to the subsystem-1. The frequency for the lumped system is defined as $\omega^2 = \frac{K}{M}$. Both the K and M is dependent on the design variable. But the change of K and M is not only dependent on x_i but also dependent on the connectivity of structure. Thus Both the connectivity and the design variables associated with it playes a role in optimizing ω^2. For this subsystem 2, the objective of maximizing the natural frequency can be written as,

$$\begin{aligned} \text{minimise:} \quad & -\omega^2 && (3.21)\\ \text{subjected to:} \quad & x^{min} - x_i \leq 0 && (3.22)\\ & x_i - 1 \leq 0 && (3.23)\\ & \sum x_i - V_f \cdot \text{nelem} \leq 0 && (3.24) \end{aligned}$$

where, ω^2 is the natural frequency. ω^2 can be found by solving the generalized eigen value problem given by

$$(\mathbf{K} - \omega^2 \mathbf{M})\mathbf{U}_\lambda = 0 \tag{3.25}$$

Where $\mathbf{U}_\lambda$ is the eigen vector associated with the particular natural frequency. The design variable x_i's are implicitly linked to the objective though $\mathbf{K}$ and $\mathbf{M}$ matrix. Now taking the derivative with respect to a design variable x_i leads to

$$(\mathbf{K} - \omega^2 \mathbf{M})\frac{\partial \mathbf{U}_\lambda}{\partial x_i} + \frac{\partial \mathbf{K}}{\partial x_i}\mathbf{U}_\lambda - \frac{\partial \omega^2}{\partial x_i}\mathbf{M}\mathbf{U}_\lambda - \omega^2 \frac{\partial \mathbf{M}}{\partial x_i}\mathbf{U}_\lambda = 0 \tag{3.26}$$

Multiplying the vector equation with $\mathbf{U}_\lambda^T$ leads to the first term to go to 0 which on further simplifying the expression gives

$$\frac{\partial \omega^2}{\partial x_i} = \frac{\mathbf{U}_\lambda^T \frac{\partial \mathbf{K}}{\partial x_i}\mathbf{U}_\lambda - \omega^2 \mathbf{U}_\lambda^T \frac{\partial \mathbf{M}}{\partial x_i}\mathbf{U}_\lambda}{\mathbf{U}_\lambda^T \mathbf{M}\mathbf{U}_\lambda} \tag{3.27}$$

By the formulation,we can see that a single design variable x_i is associated with only one element so that each design variable are decoupled. so we can write

$$\frac{\partial \omega^2}{\partial x_i} = \frac{\mathbf{u}_\lambda^T \frac{\partial \mathbf{k}_i}{\partial x_i}\mathbf{u}_\lambda - \omega^2 \mathbf{u}_\lambda^T \frac{\partial \mathbf{m}_i}{\partial x_i}\mathbf{u}_\lambda}{\mathbf{u}_\lambda^T \mathbf{m}_i \mathbf{u}_\lambda} \tag{3.28}$$

where the $\mathbf{k}_i$ and $\mathbf{m}_i$ are element stiffness matrix. This will allow us to compute the gradient efficiently by taking the derivative of element level matrices and not the whole structure matrices. This is the gradient of the natural frequency with respect to the design variables. During the Finite element analysis, the frequency of the structure is found using

$$\omega^2 = \frac{\mathbf{U}_\lambda^T \mathbf{K} \mathbf{U}_\lambda}{\mathbf{U}_\lambda^T \mathbf{M} \mathbf{U}_\lambda} \tag{3.29}$$

The gradient value calculated in eq. (3.28) coupled with robust line-search is used to update the design variable as given in eq. (3.18).

3.5 Combined System

In the combined system we need to achieve both the targets i.e the objective of both the subsystems together. This means that the scanner should scan for deeper depths with higher frequency for collecting large data within a small time efficiently. Physically looking into this, both the subsystem level objective have a trade-off with each other. This means maximizing the displacement at a particular node (the objective of subsystem-1) will demand decrease in stiffness and maximizing the natural frequency (the objective of subsystem-2) will demand increase in the stiffness to mass ratio. We formulate the multi-objective problem into a single objective function by multiplying sub-system level objective with one another as given in eq. (3.30). Since, the system and sub-system has same design variables our linking and shared variables are all of the design variables. Thus, the lower and upper bound for the design variables, and the volume constraint also remains the same.

$$\begin{aligned}
\text{minimise f}: \quad & -\frac{MPE^m \cdot \omega^2}{SE^n} && (3.30)\\
\text{subjected to}: \quad & x^{min} - x_i \leq 0 && (3.31)\\
& x_i - 1 \leq 0 && (3.32)\\
& \sum x_i - V_f \cdot \text{nelem} \leq 0 && (3.33)
\end{aligned}$$

Since it takes less efforts to solve the complete problem we decided to go with All-In-One (AIO) strategy instead of breaking the problems in subsystems. The gradient of the function is defined as

$$\frac{\partial f}{\partial x_i} = -\frac{MPE^m}{SE^n}\frac{\partial \omega^2}{\partial x_i} + \omega^2 \frac{\partial L}{\partial x_i} \tag{3.34}$$

where $\frac{\partial L}{\partial x_i}$ and $\frac{\partial \omega^2}{\partial x_i}$ are given by eqs. (3.20) and (3.28) respectively.

4 Numerical implementation

4.1 Pre-processing

The optimization program was implemented in MATLAB and the process flow of the code is described in the fig . First we discretize the domain using small beam elements and write all information related to model in four input files as node.dat, elem.dat, dispbc.dat and forces.dat. Each row of node.dat file contains the node number and its cartesian coordinate (nx ny nz), and the nodal force are mentioned in the forces.m file. Each row of elem.dat file represents a beam element, and contains the elements number, nodes associated with that element, width, thickness, Youngs modulus, and direction vector of width. These three files are then read by script file beamOptMerge.m to build the FEA model. The rows of dispbc.m file represents the boundary condition to be applied at specified node, which are read by script file and converted to format that can be passed to the FEA solver (filename feasolver.m). Refer section 5.1 for an example.

4.2 Optimisation

Once we built the geometrical model, we specify all the parameters and stopping criteria to be used by optimization solver fmincon. Fmincon is a inbuilt MATLAB function that solves the optimization problem specified in negative null form. We use fmincon as it is capable of handling linear and nonlinear constraints, as well as equality and inequality constraints. We formulate the volume constraints as given in eq. (3.24). We then initialize the design, create FEA solver handle and pass all the relevant information to the fmincon. Fmincon solves the optimisation problem using SQP with user specified gradient information. fmincon passes intermediate design variables to FEA solver to get the objective function and its gradient value.

The optimisation strategy mentioned above sometimes generated disconnected members. This problem can be overcome by using a filtering scheme

as proposed by Sigmund [2], that prevents rapid variation in gradient of objective function in the neighborhood. For an element, i, neighboring elements are first identified within a circular region of radius, r_{min} about the considered element i. The number of neighboring elements $k(i)$ is a function of i-th eleement.

$$\begin{aligned} H^j &= r_{min} - \text{dist(i,j)}, \quad \{i \in N \mid \text{dist(i,j)} \leq r_{min}\} \\ i &= 1, \cdots, N, \\ j &= 1, \cdots, k(i), \end{aligned} \tag{4.1}$$

$$gradient^f(i) = \frac{1}{x_i \sum_{j=1}^{k(i)} H^j} \sum_{j=1}^{k(i)} H^j \frac{\partial f}{\partial x_j} \tag{4.2}$$

where dist(i,j) is defined as the distance between the center of the neighboring element, j and the considered element, i. $gradient^f(i)$ represents the filtered value of gradient.

4.3 Post-processing: Binary filtering

The concept of filtering is based on the lower and upper bound on design variables. Ideally, the design variable should be either 0 or 1 as it represents the presence or absence of the element. As we have discussed earlier, having the lower bound for design variable as 0 will create instability in FE analysis thus, we are providing it with a lower limit residual value. Thus, it implies that the elements having the residual values are not important and are to be removed from the structure.

Further, since this is a continuous optimization the design variable can have values between x^{min} and x^{max}. But practically this doesnt make sense because we cannot have any values of stiffness and density for the element which is a part of the large structure. Once the material is chosen for the structure, either the material can be present or absent. Thus it leads to the fact that when the design variables have the values which are greater than some threshold we assume that the material is present (in which case the values of that particular design variables are set to 1) and for all other cases, the material is assumed to be absent. This technique of setting the design variables to either o or 1 is called binary filtering and it is used to generate the realisable optimized topology from the uncleaned model.

4.4 Process flow

The following diagram shows the process flow followed during the optimisation process as described in the above sections:

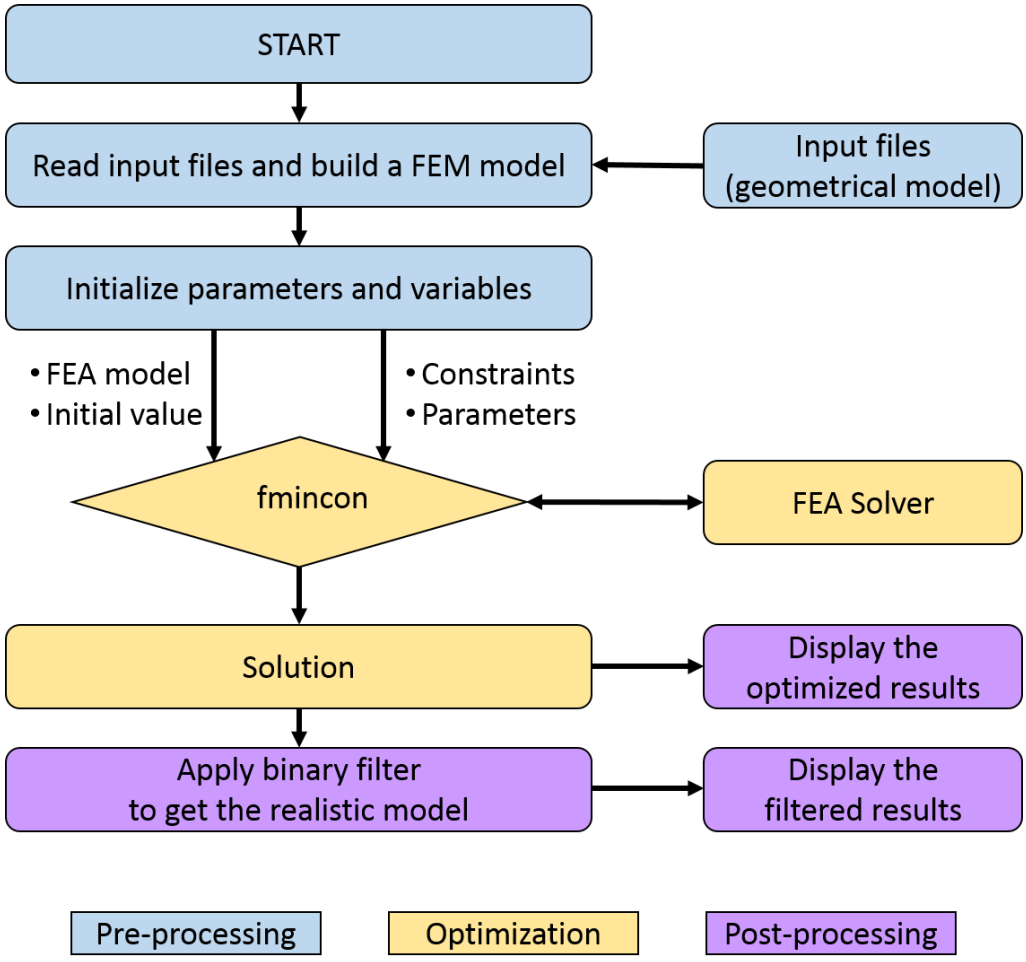

Figure 4.1: Porcess flow

5 Results

5.1 Test structure

The optimisation strategy formulated in chapter 3 is validated using a test structure as described below. We mesh a square domain of $2mm \times 2mm$ with 28 beam elements as shown in fig. 5.1. The number in parentheses indicates the element number, whereas node numbers are given in blue color. The structure is fixed at four vertices of the domain, i.e at node 1,3,7, and 9 where we constrain all translation and two in-plane rotation DOF to zeros.

$$U_x = U_y = U_z = \theta_x = \theta_y = 0$$

Various parameter and material property used to build the FEM model are tabulated in table 5.1. In this project, to start with, we try to optimise the topology such that on applying force at node 4 in the -x direction, the nodal displacement of node 6 in x-direction should be maximum.

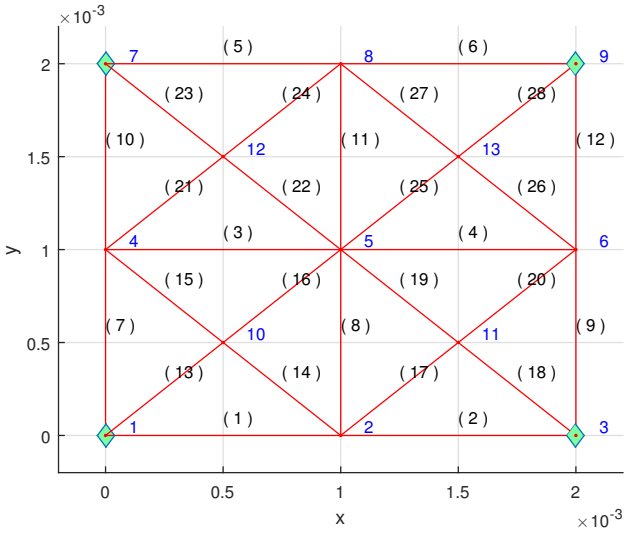

Figure 5.1: Test structure

Property name	value
Youngs' Modulus (E)	90 Mpa
Density (ρ)	3000 kg/m^3
Width (b)	70 μm
Thickness (t)	1 μm
Poisson's ratio (ν)	0.3

Table 5.1: Material properties and geometrical parameters

5.2 Optimised structure

The test structure described above is optimised for system and sub-system level and results are summarised below. The figures in gray scale shows the relative value of the design variable, where the dark color implies higher value of x_i and vice versa.

5.2.1 Sub-system 1

The geometry shown in figs. 5.2 and 5.3 was found to be best, for the given optimisation problem. The results were arrived after going through multiple iterations by changing various tuning parameters. The optimised geometry shows the displacement of 172μm on application of -5×10^{-3}N of the force. However, when we realise the actual structure, by deleting the beam members whose value was bounded by lower bound x^{min}, the total displacement is reduced to 65μm. Also, as the structure becomes more compliant the natural frequency is reduced from 5725 to 2560 rad/sec, as seen from the table 5.2. The parameters used to get the results are tabulated in table 5.3

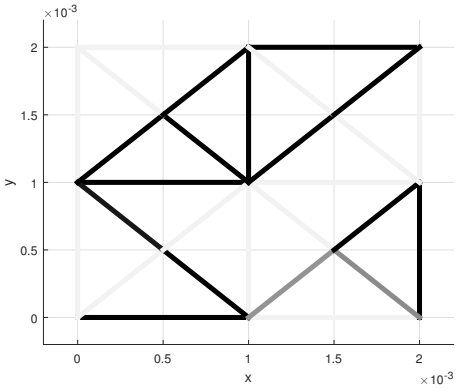

Figure 5.2: Optimised geometry 1

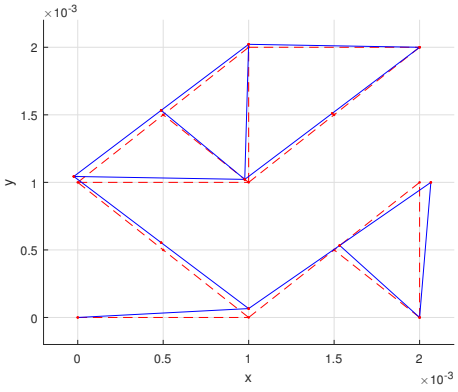

Figure 5.3: Filtered geometry 1

Function	Base geometry	Optimised geometry	Filtered geometry
MPE = U_B (μm)	-0.14	172	65.91
MPE/SE	-82.3	1170	1150
ω (rad/sec)	5725	2560	2527

Table 5.2: Results for sub-system1

Parameters	value	Parameters	value
p	3	m	1
q	1	n	1
$\mathbf{X}_0$	**0.5**	Force	-5×10^{-3}N
V_f [1]	0.5	filter	2

Table 5.3: Parameter for sub-system 1 and 2

The complexity of the topology can be reduced if we restrict the total volume to a small value by putting volume constrain. The results for volume fraction $V_f = 0.2$, and p = q = m = n = 1, are shown in the figs. 5.4 and 5.5. The displacement U_B for the filtered geometry is equal to $50\mu m$, which is comparable to best possible topology mentioned above.

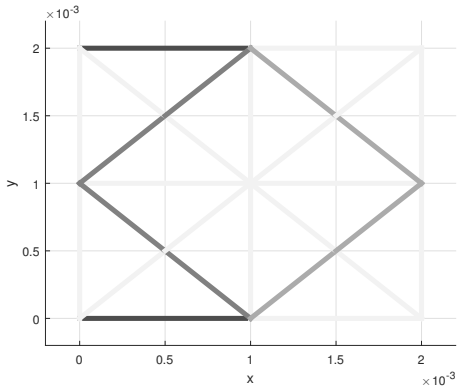

Figure 5.4: Optimised geometry with volume constraint

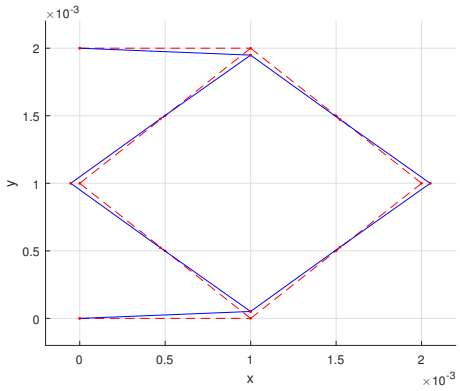

Figure 5.5: Filtered geometry with volume constraint

Further, to see the effect of mesh refinement on the results, the optimization was carried out with refined mesh and similar trends were observed. The results are shown below:

[1] volume constraint only used in sub-system 2

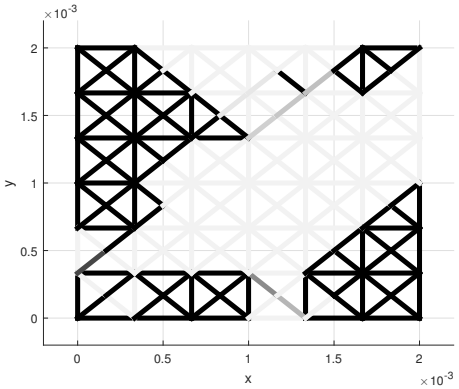

Figure 5.6: Optimised geometry using fine mesh

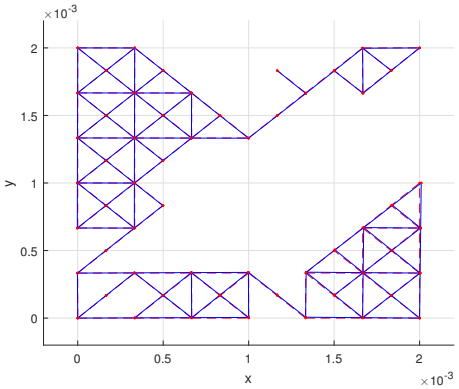

Figure 5.7: Filtered geometry using fine mesh

5.2.2 Sub-system 2

The subsystem -2 is optimised by taking the test structure as shown in fig. 5.1. The input values are given in table 5.3. It is generally a convention to start the topology optimization by initializing the design variables to half the value between the lower bound and upper bound. So all the design variable has been initialised to 0.5. Further the SIMP parameters are set to p=3, q=1 with the volume constraint being half of the maximum possible volume (refer table 5.3). The optimized topology is shown in fig. 5.8. This optimized body shows how the topology should be. The filter scheme is used to retrieve the optimized topology for the body by removing unwanted elements. The filtered topology of the structure is shown in fig. 5.9.

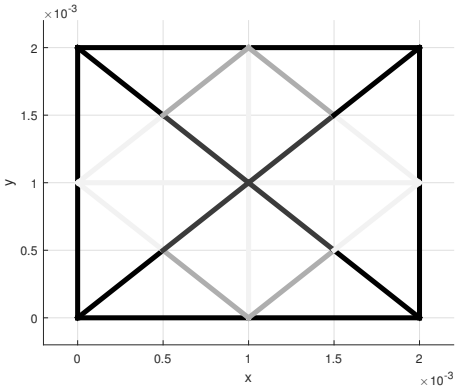

Figure 5.8: Optimised geometry 2

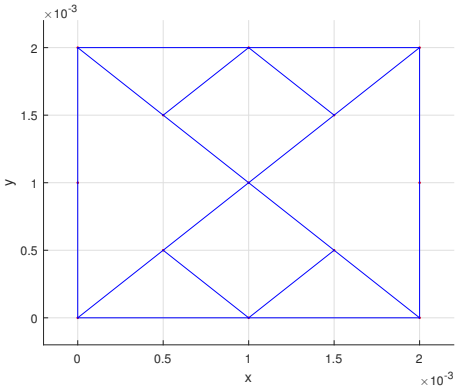

Figure 5.9: Filtered geometry 2

Function	Base geometry	Optimised geometry	Filtered geometry
MPE = U_B (μm)	−0.14	18.4	13.5
MPE/SE	−82.3	49.1	40
ω (rad/sec)	5725	7810	7280

Table 5.4: Results for sub-system 2

In the table 5.4 the optimized results are those which are generated by optimization code and the filtered results are those which are generated by applying filtering scheme to the optimized results to generate a feasible topology. We see that frequency is significantly improved from 5.7 kHz to 7.8 kHz which is around 36% improvement from the base structure. Further while filtering, the objective function (frequency) reduces slightly. This is due to the fact that some unimportant materials are being removed while filtering, which reduces the stiffness of the structure. The same analysis is performed in a fine mesh with the same inputs. The topology optimized using the fine mesh is shown below

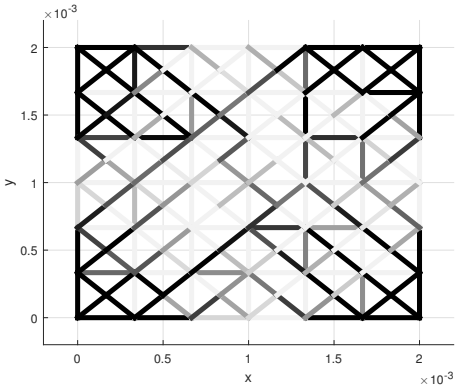

Figure 5.10: Optimised geometry with fine mesh

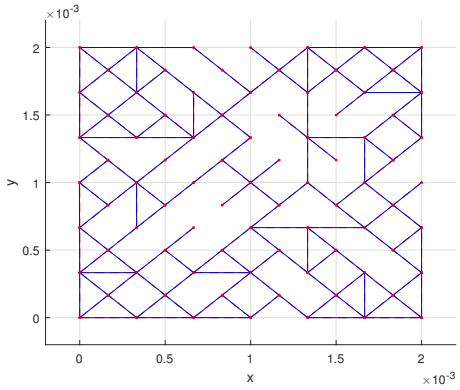

Figure 5.11: Filtered geometry with fine mesh

5.2.3 System

The topology which is shown in fig. 5.12 and fig. 5.13 was the best for combined formulation of objective function as given in eq. (3.30). Similar to subsystem -1 and subsystem-2 results were arrived after performing series of experiments with different parameters. The results are tabulated in table 5.5

Function	Base geometry	Optimised geometry	Filtered geometry
MPE = U_B (μm)	-0.14	62	21
ω^2 MPE/SE	4.71×10^5	2.79×10^6	2.45×10^6
ω (rad/sec)	5725	6450	6010

Table 5.5: Results for sub-system 2

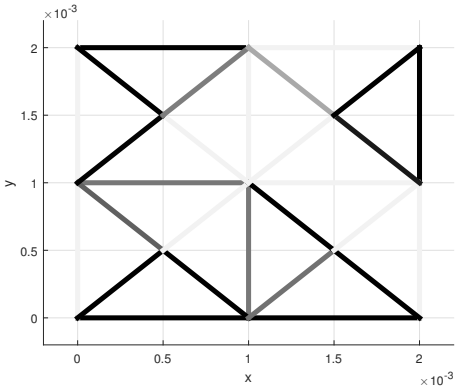

Figure 5.12: Optimised geometry for combined system

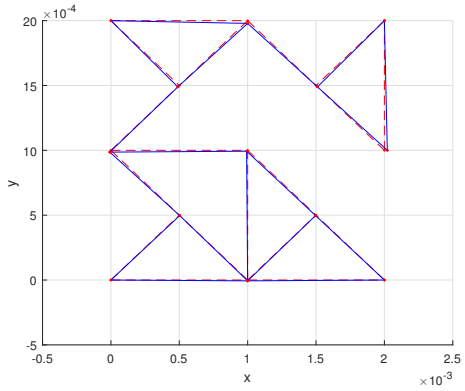

Figure 5.13: Filtered geometry for combined system

Further, the same optimization procedure is done using fine mesh and the results are shown in fig. 5.14 and fig. 5.15

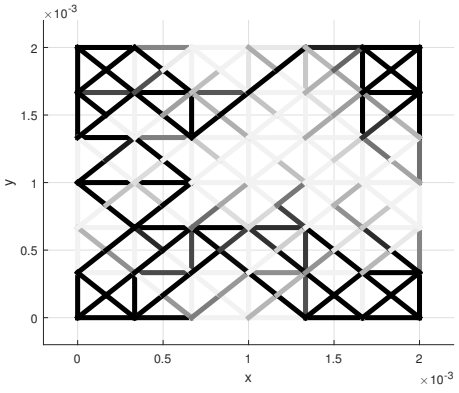

Figure 5.14: Optimised geometry using fine mesh for combined system

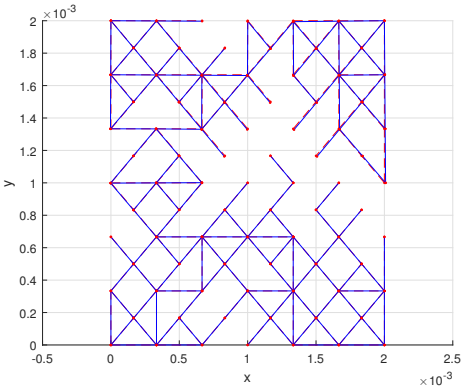

Figure 5.15: Filtered geometry using fine mesh for combined system

5.3 Parametric and sensitivity analysis

Parametric study is done to find the effect of change in parameter value on the objective function and the optimised topology. Few of the observations made during this study are listed below

1. The study at system level and sub-system level reveals that changing initial value of design variable has no effect on the optimization results. This is done by iterating the same problem by varying the initial values of design variables from 0.2 to 0.7.

2. In sub-system1, volume constraint is active only when bounded by small volume ($V_f \leq 0.4$), however in sub-system2 it is active for even larger values of V_f. Further when the volume constraint is gradually relaxed the objective function gradually improves. This analysis is done by having different V_f ranging from 0.2 to 0.7.

3. For sub-system1, the lagrange multiplier was found to be 28 for $V_f = 0.2$ case. For sub-system2, the objective value for $V_f = 0.7$ is better that for volume constraint being 0.2. This is due to the fact that the physics of the model demands more volume to be put in specific places to attain maximum stiffness but the volume constraint will not allow it.

4. In sub-system2, it is also observed that $V_f \geq 0.7$ becomes inactive. This is due to the fact that after adding full volume at a very specific places to increase the stiffness, if it adds further the stiffness increase will not be that much as for like the increase in mass. In that case adding more volume after certain point will worsen the objective function. Thus at greater values of volume constraint becomes inactive.

5. The SIMP parameter p has contrast effect on sub-system 1 and 2. Increasing the value of p increases the objective function for sub-system 1, and decreases the natural frequency for sub-system2. This is because higher values of p penalises the design variable with respect to stiffness alone, making the topology more compliant and increasing the displacement. Since the mass matrix is unaffected by increasing p, the natural frequency is decreased. It has also been seen that at higher values of P with lower volume constraints creates disconnected geometry

6. Changing the mesh size from coarse to fine gives similar topology, but with better physical insight.

7. The displacement at point B, was observed to changed linearly with respect to external force, with no change in natural frequency. This is as expected, because we use a linear FEM formulation. Also, natural frequency is calculated for the unforced system, hence remains unaffected by force.

5.4 Future Work

In this optimization, we have used in plane loading which are much simpler in analysis. Further to accurately simulate the structure, we should consider out of plane loading which will involve deformations in all three directions.The bottleneck in this implementation is to ensure connectivity for 1D elements. Though there are few methods found in the literature for ensuring connectivity, those are easier to implement in 2-D elements than 1D elements. This implementation is necessary because the topology design should be connected from start to end or else it will be meaningless.

During this optimization project we have used 1-D elements for developing mathematical model. This can be extended to 2D elements which represents the physical domain more accurately. The cusp point in developing this is in generating K matrix and M matrix, which should incorporate all degrees of freedom. With this, 2D elements can be modelled by appropriately modifying few blocks in the code which we have developed.

Acknowledgments

We would like to acknowledge Prof. GK Ananthasuresh (Department of Mechanical Engineering, Indian Institute of Science, Bangalore) for using his FEM code as template to develop topology optimization code in MATLAB.

References

[1] A. Saxena and G. Ananthasuresh, "On an optimal property of compliant topologies," *Structural and multidisciplinary optimization*, vol. 19, no. 1, pp. 36–49, 2000.

[2] O. Sigmund, "On the design of compliant mechanisms using topology optimization*," *Journal of Structural Mechanics*, vol. 25, no. 4, pp. 493–524, 1997.